Activation of Arylnitroso Substrates on a Platinum−Germylene Complex Facilitating the Formation of New N−C and N−S Bonds

Kyle E. Litz, Jeffrey W. Kampf, and Mark M. Banaszak Holl*

Contribution from the Department of Chemistry, University of Michigan, Ann Arbor, Michigan 48109-1055

Received March 16, 1998

Abstract: The reaction of $(Et_3P)_2PtGe[N(SiMe_3)_2]_2$ (**1**) with nitrosobenzene and 2-nitrosotoluene yields $(Et_3P)_2$-PtN(Ph)OGe$[N(SiMe_3)_2]_2$ (**3a**) and $(Et_3P)_2PtN(o\text{-}Tol)OGe[N(SiMe_3)_2]_2$ (**3b**), respectively. The reactivity of **3a** with SO_2, H_2CO, CO_2, and PhNCO was explored yielding the five-membered heterocyclic complex $(Et_3P)_2$-PtS(O)$_2$N(Ph)OGe$[N(SiMe_3)_2]_2$ (**6a**) and the six-membered heterocyclic complexes $(Et_3P)_2PtOC(H)_2N(Ph)$-OGe$[N(SiMe_3)_2]_2$ (**7a**), $(Et_3P)_2PtOC(O)N(Ph)OGe[N(SiMe_3)_2]_2$ (**8a**), and $(Et_3P)_2PtN(Ph)C(O)N(Ph)OGe$-$[N(SiMe_3)_2]_2$ (**9a**), respectively. The structures of **3a**, **6a**, **7a**, and **9a** were determined by single-crystal X-ray diffraction. **3b** was observed to react in a fashion similar to **3a** as demonstrated by reactions with SO_2 and H_2CO which gave $(Et_3P)_2PtS(O)_2N(o\text{-}Tol)OGe[N(SiMe_3)_2]_2$ (**6b**) and $(Et_3P)_2PtOC(H)_2N(o\text{-}Tol)OGe[N(SiMe_3)_2]_2$ (**7b**). Complexes **6a** and **6b** represent the first isolated and characterized examples of metal-stabilized −S(O)$_2$N-(R)O− fragments, the isoelectronic analogue of an elusive intermediate proposed as the first step in Contact Process for the oxidation of SO_2 by platinum catalysts. As a group, the reactions in this paper demonstrate the cooperative ability of metal−germylenes to activate unsaturated organic substrates and promote their subsequent chemical modification, while avoiding scission of the Pt−Ge bond.

Introduction

The germylene ligand binds in a dative sense to electron-rich late transition metals and maintains the presence of an active Lewis acid site.[1] This combination of properties provides compelling incentive to explore the ability of the M−Ge nexus to activate a variety of small molecules and functional groups. Significant challenges to be overcome in transition metal−germylene chemistry include (1) irreversible oxidation of the germylene to a metal bound germyl and (2) uncontrolled M−Ge bond scission. Group 10 metal−germylene complexes provide a powerful combination of electronic donor and acceptor orbitals at a chemically convenient distance of separation. The strongly basic Pt^0 and Ni^0 in $(Et_3P)_2PtGe[N(SiMe_3)_2]_2$ (**1**) and $(Ph_3P)_2$-NiGe$[N(SiMe_3)_2]_2$ (**2**) are located just 2.30 and 2.21 Å, respectively, from the Lewis acidic Ge(II) atom.[2,3] This proximate pairing of metal orbitals has been shown to promote interaction with small molecules, such as CO_2, yielding novel cycloadducts. In addition, *reversible* metal−germyl formation in concert with H_2 and CO_2 activation, reversible Pt−Ge scission leading to the formation of bisaminogermane, and catalytic synthesis of amide germanes have been observed.[2,3] A variety of interesting chemical behavior has been noted in related M−Ge/Si/Sn systems.[4] Of particular relevance to work reported in this paper, Tilley et al. have recently observed the reversible cycloaddition of isocyanates on metal−silylene complexes, $[Cp^*(PMe_3)_2Ru=SiR_2]BPh_4$ (R = Me, Ph).[5]

As part of our exploration of metal−germylene chemistry, activation and subsequent modification of organic functional

groups is being examined. In this paper, we report the reaction of nitrosobenzene and 2-nitrosotoluene with **1** generating four-membered metallacyclic adducts containing an extremely lengthened N−O bond. Furthermore, a variety of insertion reactions into the nitroso-adducts have been explored.[6] A particularly interesting insertion of SO_2 forms new N−S bonds and leads to a unique complex related to a key proposed intermediate in the Contact Process.[7] Insertion products of PhNCO, H_2CO, and CO_2, leading to new N−C bonds, are also described. These reactions provide a demonstration that the metal−germylene nexus can activate unsaturated organic substrates and promote their further chemical modification.

Experimental Section

All manipulations were performed using air-free technique and dry, deoxygenated solvents. Toluene, hexane, and benzene-d_6 were degassed

(1) For reviews on germylenes, see: (a) Neumann, W. P. *Chem. Rev.* **1991,** 91, 311−334. (b) Barrau, J.; Escudie, J.; Satge, J. *Chem. Rev.* **1990,** *90,* 283−319. (c) Lappert, M. F.; Rowe, R. S. *Coord. Chem. Rev.* **1990,** *100,* 267−292. (d) Petz, W. *Chem. Rev.* **1986,** *86,* 1019−1047. (e) Tandura, S. N.; Gurkova, S. N.; Gusev, A. I. *Zh. Strukt. Khim.* **1990,** *31,* 154.

(2) Litz, K. E.; Bender, J. B.; Kampf, J. W.; Banaszak Holl, M. M. *Angew. Chem., Int. Ed. Engl.* **1997,** *36,* 496.

(3) Litz, K. E.; Henderson, K. H.; Gourley, R. W.; Banaszak Holl, M. M. *Organometallics* **1995,** *14,* 5008.

(4) (a) For example, see: Koe, J. R.; Tobita, H.; Suzuki, T.; Ogino, H. *Organometallics* **1992,** *11,* 150. (b) Koe, J. R.; Tobita, H.; Ogino, H. *Organometallics* **1992,** *11,* 2479. (c) Figge, L. K.; Carroll, P. J.; Berry, D. H. *Angew. Chem., Int. Ed. Engl.* **1996,** *35,* 435. (d) Figge, L. K.; Carroll, P. J.; Berry, D. H. *Organometallics* **1996,** *15,* 209. (e) Reichl, J. A.; Popoff, C. M.; Gallagher, L. A.; Remsen, E. E.; Berry, D. H. *J. Am. Chem. Soc.* **1996,** *118,* 9430. (f) Baines, K. M.; Cooke, J. A.; Vittal, J. J. *J. Chem. Soc. Chem. Commun.* **1992,** 1484. (g) Toltl, N. P.; Leigh, W. J.; Kollegger, G. M.; Stibbs, W. G.; Baines, K. M. *Organometallics* **1996,** *15,* 3732. (h) Sharma, H. K.; Cervantes-Lee, F.; Parkanyi, L.; Pannell, K. H. *Organometallics* **1996,** *15,* 5, 429. (i) Sharma, S.; Cervantes, J.; Mata-Mata, J. L.; Brun, M.-C.; Cervantes-Lee, F.; Pannell, K. H. *Organometallics* **1996,** *14,* 4269. (j) Sharma, H.; Pannell, K. H. *Organometallics* **1996,** *13,* 4946. (k) Barrau, J.; Rima, G.; Cassano, V.; Satge, J. *Inorg. Chim. Acta* **1992,** 189−200, *461.* (l) Chaubon-Deredempt, M. A.; Escudie, J.; Couret, C. *J. Organomet. Chem.* **1994,** *467,* 37.

(5) Tilley, T. D.; Mitchell, G. P. *J. Am. Chem. Soc.* **1997,** *119,* 11236.

(6) Lead references into previous work in this area include (a) Pizzotti, M.; Porta, F.; Cenini, S.; Demartin, F.; Masciocchi, N. *J. Organomet. Chem.* **1987,** 330, 265. (b) Bellon, P. L.; Cenini, S.; Demartin, F.; Pizzotti, M.; Porta, F. *J. Chem. Soc., Chem. Commun.* **1982,** 265. (c) Cenini, S.; Porta, M.; Pizzotti, M.; LaMonica, G. *J. Chem. Soc., Chem. Dalton Trans.* **1984,** 355. (d) Cenini, S.; Porta, F.; Pizzotti, M.; Crotti, C. *J. Chem. Soc., Dalton Trans.* **1985,** 163. (e) Demartin, F.; Pizzotti, M.; Porta, F. *J. Chem. Soc., Dalton Trans.* **1987,** 605.

(7) For lead references into the area of homogeneous SO_2 oxidation, see: Kubas, G. J. *Acc. Chem. Res.* **1994,** *27,* 183.

and dried over sodium benzophenone ketyl. Chloroform was degassed and stored over 4 Å molecular sieves. Chloroform-*d* was used as received from Cambridge Isotopes. PhNO, 2-nitrosotoluene, *N*-nitrosodimethylamine, 2,4,6-tri-*tert*-butylnitrosobenzene, paraformaldehyde, and dimethylacetylene dicarboxylate (Aldrich Chemical) were degassed in vacuo and stored under dinitrogen in a drybox. The following complexes were prepared according to previously published procedures: $(Et_3P)_2PtGe[N(SiMe_3)_2]_2$ (**1**),[3] $(Ph_3P)_2NiGe[N(SiMe_3)_2]_2$ (**2**),[2] $(Et_3P)_2PtO_2C^{13}O$,[8] and $Ge[N(SiMe_3)_2]_2$.[9] ^1H, ^{13}C, and ^{31}P NMR spectra were obtained in the listed deuterated solvents on a Bruker AM-360 spectrometer (360.1, 90.6, and 145.8 MHz) and referenced to residual protons, solvent carbons, and external 85% H_3PO_4 in D_2O, respectively. IR spectra were recorded on a Nicolet 5DXB as Nujol mulls or KBr disks. All compounds reported are moisture sensitive to hydrolysis reactions of the $Ge[N(SiMe_3)_2]_2$ ligand.

$(Et_3P)_2PtN(Ph)OGe[N(SiMe_3)_2]_2$ (3a). To a stirring, cold (-78 °C) 25 mL toluene solution of **1** (0.01 M) was added 0.025 g (0.24 mmol) of PhNO via a solids addition tube. The color darkened from yellow to amber at -50 °C. After 3 h at -11 °C, the dark orange solution was filtered, and the toluene was removed in vacuo leaving a dark red oil. Recrystallization from a minimum of cold hexane at -78 °C and drying in vacuo gave 0.120 g of an orange precipitate (51% isolated yield). The thermally stable solid was observed to be light sensitive, decomposing over a period of several days. X-ray quality crystals were obtained by slow evaporation of a benzene solution. ^1H NMR (C_6D_6) δ 0.62 (s, 36H, N(SiMe$_3$)$_2$), 0.82 (m, 18H, CH$_2$CH_3), 1.49 (m, 6H, CH_2CH$_3$), 1.70 (m, 6H, CH_2CH$_3$), 6.63 (1H, aromatic), 7.09 (2H, aromatic), 7.27 (2H, aromatic); ^{13}C NMR (C_6D_6) δ 7.54 (s, N(SiMe$_3$)$_2$), 8.31 (d, CH$_2$CH$_3$), 8.97 (d, CH$_2$CH$_3$), 18.24 (m, CH$_2$CH$_3$), 21.30 (m, CH$_2$CH$_3$), 113.74 (s, aromatic), 115.88 (s, aromatic), 127.73 (s, aromatic) other is obscured by solvent; ^{31}P NMR (C_6D_6) δ -9.23 (d w/^{195}Pt satellites, $^2J_{P-P} = 16.8$ Hz, $^1J_{P-P} = 3021$ Hz), 4.44 (d w/^{195}Pt satellites, $^2J_{P-P} = 16.8$ Hz, $^1J_{Pt-P} = 1888$ Hz). Elemental analysis for $C_{30}H_{71}N_3GeOP_2PtSi_4$: C, 38.67, H, 7.68; N, 4.51. Found: C, 38.62, H, 7.57, N, 4.55.

$(Et_3P)_2PtN(o\text{-}Tol)OGe[N(SiMe_3)_2]_2$ (3b). In the same fashion as **3a**, 0.037 g (0.31 mmol) of 2-nitrosotoluene was added to a toluene solution of **1** (0.250 g, 0.30 mmol) at -78 °C. An amber hue developed at -10 °C. After stirring for 3 h (11 °C), the solution was filtered, and the solvent was removed in vacuo leaving a dark red oil. Recrystallization from a minimum of cold hexane at -78 °C and drying in vacuo gave 0.118 g (41% isolated yield) of an orange solid. The thermally stable solid was observed to be light sensitive, decomposing over a period of several days. ^1H NMR (C_6D_6) δ 0.53 (broad, 18H, N(SiMe$_3$)$_2$), 0.70 (broad, 18H, N(SiMe$_3$)$_2$), 0.83 (m, 18H, CH$_2$CH_3), 1.16 (m, 3H, CH_2CH$_3$), 1.30 (m, 3H, CH_2CH$_3$), 1.70 (m, 6H, CH_2-CH$_3$), 2.75 (s, 3H, tol-CH_3), 6.96 (1H, aromatic), 7.10 (1H, aromatic), 7.18 (1H, aromatic); 7.55 (1H, aromatic); ^{13}C NMR (C_6D_6) δ 7.91 (s, N(SiMe$_3$)$_2$), 8.97 (d, CH$_2$CH_3), 16.7 (m, CH$_2$CH$_3$), 20.2 (s, tol-CH$_3$) 21.2 (m, CH$_2$CH$_3$), 122.1 (s, aromatic), 123.8 (s, aromatic), 126.7 (s, aromatic), 130.6 (s, aromatic), 136.0 (aromatic quaternary to methyl), 160 (N−C quaternary aromatic); ^{31}P NMR (C_6D_6) δ -7.24 (d w/^{195}Pt satellites, $^2J_{P-P} = 15.4$, $^1J_{P-P} = 2794$ Hz), 8.00 (d w/^{195}Pt satellites, $^2J_{P-P} = 15.1$ Hz, $^1J_{Pt-P} = 1914$ Hz); Elemental analysis for $C_{31}H_{73}N_3$-GeOP$_2$Si$_4$: C, 39.36, H, 7.78; N, 4.44. Found: C, 39.04; H, 7.71; N, 4.44.

$(Et_3P)_2PtS(O)_2N(Ph)OGe[N(SiMe_3)_2]_2$ (6a). A 15 mL toluene solution of **3a** (0.142 g, 0.15 mmol) was generated as described above. SO_2 (0.15 mmol) was condensed via a measured gas bulb into the stirring -78 °C solution of crude **3a** causing an immediate color change to light yellow. The solution was warmed to room temperature over 3 h followed by removal of all volatiles in vacuo. Extraction with a minimum (0.5 mL) of THF under an inert atmosphere followed by addition of $\sim$0.1 mL diethyl ether resulted in large, colorless crystals of **6** over 24 h. The collected crystals were washed with 2 × 0.5 mL of diethyl ether leaving 102 mg (66% isolated yield) of **6a**. **6a** was

found to be insoluble in diethyl ether and pentane, yet displayed limited solubility in benzene and toluene; it was quite soluble in chloroform and THF. ^1H NMR (C_6D_6) δ 0.60 (broad s, 36H, N(SiMe$_3$)$_2$), 0.72 (m, 9H, CH$_2$CH_3), 0.83 (m 9H, CH$_2$CH_3), 1.82 (m, 6H, CH_2CH$_3$), 1.86 (m, 6H, CH_2CH$_3$), 6.99 (1H, aromatic), 7.27 (2H, aromatic), 8.12 (2H, aromatic); ^{13}C NMR (CDCl$_3$) δ 7.19 (s, SiMe$_3$), 8.10 (d, PCH$_2$CH$_3$), 9.18 (d, PCH$_2$CH$_3$), 16.23 (m, PCH$_2$CH$_3$), 20.03 (m, PCH$_2$CH$_3$), 124.16 (s, aromatic), 124.85 (s, aromatic), 127.67 (s, aromatic), 141.78 (s, N−C aromatic); ^{31}P NMR (CDCl$_3$) δ 7.15 (d w/^{195}Pt satellites, $^1J_{P-P} = 2025$ Hz, $^2J_{P-P} = 22$ Hz), -6.48 (d w/^{195}Pt satellites, $^1J_{P-P} = 2866$ Hz, $^2J_{P-P} = 22$ Hz); IR (Kbr) 1384 (asym ν-SO$_2$), 1165 (sym ν-SO$_2$); Elemental analysis for $C_{30}H_{71}N_3GeO_3P_2SSi_4Pt$: C, 36.18, H, 7.19; N, 4.22. Found: C, 37.65; H, 6.89; N, 3.74.

$(Et_3P)_2PtS(O)_2N(o\text{-}Tol)OGe[N(SiMe_3)_2]_2$ (6b). SO_2 (1 equiv) was condensed from a measured gas bulb into a frozen 0.25 mL C_6D_6 solution of **3b** (60 mg, 0.063 mmol) in an NMR tube fitted with a Teflon valve. After sealing the tube, the solution was rapidly thawed resulting in an immediate color change from dark orange to colorless. Complete conversion to **6b** was demonstrated by NMR analysis. ^1H NMR (C_6D_6) δ 0.48 (s, 9H, N(SiMe$_3$)$_2$), 0.53 (s, 9H, N(SiMe$_3$)$_2$), 0.67 (s, 9H, N(SiMe$_3$)$_2$), 0.81 (s, 9H, N(SiMe$_3$)$_2$), 0.83 (m, 18H, CH$_2$CH_3), 1.86 (m, 12H, CH_2CH$_3$), 2.90 (s, 3H, tol-CH_3), 7.01 (m, 1H, aromatic), 7.16 (s, 1H, aromatic), 7.21 (d, 1H, aromatic); 8.28 (d, 1H, aromatic); ^{13}C NMR (C_6D_6) δ 6.79 (s, SiMe$_3$), 7.49 (s, SiMe$_3$), 7.69 (d, SiMe$_3$), 7.94 (d, SiMe$_3$), 8.69 (m, PCH$_2$CH$_3$), 16.15 (m, PCH$_2$CH$_3$), 19.80 (m, PCH$_2$CH$_3$), 20.60 (s, Aromatic-*Me*), 125.1 (s, aromatic), 126.1 (s, aromatic), 127.8 (s, aromatic), 130.5 (s, aromatic), other aromatic carbons too weak to detect at this concentration; ^{31}P NMR (C_6D_6) δ 8.89 (d w/^{195}Pt satellites, $^1J_{P-P} = 2042$ Hz, $^2J_{P-P} = 23$ Hz), -4.14 (d w/^{195}Pt satellites, $^1J_{Pt-P} = 2757$ Hz, $^2J_{P-P} = 23$ Hz); IR (KBr) 1384 cm^{-1}, (ν asym SO$_2$), 1181 cm^{-1} (ν sym. SO$_2$).

$(Et_3P)_2PtOC(H_2)N(Ph)OGe[N(SiMe_3)_2]_2$ (7a). Paraformaldehyde (71 mg, 0.79 mmol of H$_6$C$_3$O$_3$) was added to a stirring 5 mL C_6H_6 solution of **3a** (210 mg, 0.22 mmol) under argon in a darkened vessel. After 1 h, filtration from excess unreacted paraformaldehyde followed by recrystallization from pentane gave 123 mg of a tan powder (58% isolated yield). ^1H NMR (C_6D_6) δ 0.69 (s, 36H, Si(CH_3)$_3$), 0.78 (m, 9H, CH$_2$CH_3), 0.88 (m, 9H, CH$_2$CH_3), 1.50 (m, 6H, CH_2CH$_3$), 1.73 (m, 6H, CH_2CH$_3$), 5.11 (broad d w/^{195}Pt satellites, $^4J_{P-H} = 6.8$ Hz, $^3J_{Pt-H} = 56$ Hz, 2H, CH_2O), 6.90 (1H, aromatic), 7.30 (2H, aromatic), 7.63 (2H, aromatic); ^{13}C NMR (C_6D_6) δ 153.1 (s, ipso-Ph), 127 (s, aromatic), 121.8 (s, para-Ph), 119.9 (s, ortho-Ph), 93.3 (s, form) 19.2 (m, CH$_2$CH$_3$), 14.2 (m, CH$_2$CH$_3$), 8.65 (m, CH$_2$CH$_3$), 8.37 (m, CH$_2$CH$_3$), 7.74 (s, Si(CH$_3$)$_3$); $^{31}P\{^1H\}$ NMR (C_6D_6) δ 19.11 (d, w/^{195}Pt satellites, $^1J_{P-P} = 1859$ Hz, $^2J_{P-P} = 15.8$ Hz), -7.5 (d w/^{195}Pt satellites, $^1J_{P-P} = 3508$ Hz, $^2J_{P-P}$ 15.8 Hz); IR (KBr) 1244 ν(C−O), 899/878/857 cm^{-1} (vs) ν(Ge/Si−N); Elemental Analysis Calcd for $C_{31}H_{73}GeN_3O_2P_2PtSi_4$: C, 38.71; H, 7.65; N, 4.37. Found C, 38.32; H, 7.41; N, 4.08.

$(Et_3P)_2PtOC(H_2)N(o\text{-}Tol)OGe[N(SiMe_3)_2]_2$ (7b). Paraformaldehyde (5 mg, 0.16 mmol) was allowed to react with 0.020 g (0.02 mmol) of **3b** in an NMR tube. After 1 h complete conversion to **7b** occurred. ^1H NMR (C_6D_6) δ 0.70 (s, 36H, N(SiMe$_3$)$_2$), 0.78 (m, 18H, CH$_2$CH_3), 1.50 (m, 6H, CH_2CH$_3$), 1.74 (m, 6H, CH_2CH$_3$), 2.53 (s, 3H, tol-CH_3), 4.75 (broad d w/^{195}Pt satellites, $^4J_{P-H} = 8$ Hz, $^3J_{Pt-H} = 47$ Hz, 2H, CH_2O), 6.98 (m, 1H, aromatic), 7.12 (s, 1H, aromatic), 7.35 (d, 1H, aromatic); 8.32 (d, 1H, aromatic).

$(Et_3P)_2PtOC(O)N(Ph)OGe[N(SiMe_3)_2]_2$ (8a). A 10-fold excess of 20% $^{13}CO_2/ CO_2$ was condensed into an NMR tube containing 100 mg (0.11 mmol) of **3a** dissolved in 0.25 mL of C_6D_6. The solution quickly lightened from dark orange to light orange within an hour. ^1H NMR (C_6D_6) δ 0.57 (s, 36H, Si(CH_3)$_3$), 0.70 (m, 9H, CH$_2$CH_3), 0.90 (m, 9H, CH$_2$CH_3), 1.69 (m, 6H, CH_2CH$_3$), 1.79 (m, 6H, CH_2CH$_3$), 6.95 (t, para-aromatic), 7.35 (t, meta-Ph), 7.99 (d, ortho-Ph); ^{13}C NMR (C_6D_6) δ 161.46 (d, $^{13}CO_2$, $^3J_{P-C} = 2.4$ Hz), 128.53 (s, aromatic), 124.71 (s, aromatic), 123.03 (s, aromatic), 122.63 (s, aromatic) 20.07 (m, CH$_2$-CH$_3$), 14.6 (m, CH$_2$CH$_3$), 9.08 (m, CH$_2$CH$_3$), 8.33 (m, CH$_2$CH$_3$), 7.23 (s, Si(CH$_3$)$_3$); $^{31}P\{^1H\}$ NMR (C_6D_6) δ 20.18 (d, w/^{195}Pt satellites, $^1J_{Pt-P} = 1873$ Hz, $^2J_{P-P} = 18.6$ Hz), -10.25 (d w/^{195}Pt satellites, $^1J_{Pt-P} = 4014$ Hz, $^2J_{P-P}$ 17.4 Hz); IR (solution in toluene/NaCl cell; mode, cm^{-1},

(8) Prepared according to the silver (I) carbonate route described: Hayward, P. J.; Blake, D. M.; Wilkinson, G.; Nyman, C. J. *J. Am. Chem. Soc.* **1970**, 92, 5873−5878.

(9) Gynane, M. J. S.; Harris, D. H.; Lappert, M. F.; Power, P. P.; Riviere, P.; Riviere-Baudet, M. *J. Chem. Soc., Dalton Trans.* **1977**, 2004−2009.

Table 1. Summary of Crystallographic Data for **3a**, **6a**, **7a**, and **9a**

compound	**3a**	**6a**	**7a**	**9a**
empirical formula	$C_{30}H_{71}GeN_3OP_2PtSi_4$	$C_{33}H_{70}GeN_3O_3P_2PtSSi_4 \cdot 3C_6H_6$	$C_{34}H_{76}GeN_3O_2P_2PtSi_4 \cdot C_6H_6$	$C_{46}H_{65}GeN_4O_2P_2PtSi_4 \cdot 1.5C_6H_6$
formula weight	931.87	1265.30	1079.07	1253.17
temperature	178(2) K	158(2) K	158(2) K	153(2) K
wavelength	0.71073 Å	0.71073 Å	0.71073 Å	0.71073 Å
crystal system	monoclinic	orthorhombic	triclinic	monoclinic
space group	$C2/c$	$Pna2_1$	$P\bar{1}$	$P2_1/c$
unit cell dimensions	$a = 42.928(3)$ Å	$a = 20.34440(10)$ Å	$a = 14.34090(1)$ Å	$a = 15.2784(4)$ Å
	$b = 11.3730(10)$ Å	$b = 21.5072(4)$ Å	$b = 18.0504(3)$ Å	$b = 16.9614(4)$ Å
	$c = 19.3500(10)$ Å	$c = 44.4859(6)$ Å	$c = 20.9629(3)$ Å	$c = 22.1374(6)$ Å
	$\alpha = 90°$	$\alpha = 90°$	$\alpha = 113.7360(10)°$	$\alpha = 90°$
	$\beta = 115.326°$	$\beta = 90°$	$\beta = 91.0210(10)°$	$\beta = 104.7243(8)°$
	$\gamma = 90°$	$\gamma = 90°$	$\gamma = 90.8190°$	$\gamma = 90°$
volume, Z	8539.5(11) Å^3, 8	19464.9(5) Å^3, 16	4965.26(11) Å^3, 4	5548.4(2) Å^3, 4
density (calculated)	1.450 mg/cm^3	1.407 mg/cm^3	1.366 mg/cm^3	1.374 mg/cm^3
absorption coefficient	4.190 mm^{-1}	3.728 mm^{-1}	3.680 mm^{-1}	3.241 mm^{-1}
F(000)	3808	8400	2052	2324
crystal size	0.18 × 0.22 × 0.44 mm	0.12 × 0.19 × 0.42 mm	0.14 × 0.24 × 0.30 mm	0.34 × 0.20 × 0.20 mm
θ range	2.80−26°	2.20−29.32°	2.12−29.04°	1.38−31.97°
limiting indices	$-52 \le h \le 47, -1 \le k \le 14,$ $-1 \le l \le 23$	$-27 \le h \le 27, -29 \le k \le 24,$ $-60 \le l \le 52$	$-18 \le h \le 15, -24 \le k \le 23,$ $-27 \le l \le 27$	$-22 \le h \le 14, -25 \le k \le 24,$ $-31 \le l \le 30$
reflections collected	10081	174787	41206	48663
independent reflections	8354 [R(int) = 0.0607]	46937 [R(int) = 0.0838]	22349 [R(int) = 0.1189]	17097 [R(int) = 0.0648]
absorption correction	XABS2	SADABS	SADABS	SADABS
max. and min. transmission	1.256 and 0.787	0.831 and 0.597	0.831 and 0.417	0.928 and 0.629
refinement method	full-matrix least-squares on F^2	full-matrix-block least-squares on F^2	full-matrix least-squares on F^2	full-matrix least-squares on F^2
data/restraints/param	8340/0/400	46747/13/1742	22349/60/885	17095/0/555
goodness-of-fit on F^2	0.873	1.136	0.921	0.948
final R indices [$I > 2\sigma(I)$]	R1 = 0.0369, wR2 = 0.0768	R1 = 0.0653, wR2 = 0.1131	R1 = 0.0729, wR2 = 0.1627	R1 = 0.0518, wR2 = 0.1099
R indices (all data)	R1 = 0.0661, wR2 = 0.0816	R1 = 0.0934, wR2 = 0.1250	R1 = 0.1102, wR2 = 0.1737	R1 = 0.0748, wR2 = 0.1239
largest diff peak and hole	1.684 and −1.392 eÅ^{-3}	2.254 and −1.115 eÅ^{-3}	5.920 and −2.937 eÅ^{-3}	2.978 and −4.336 eÅ^{-3}

and rel intensity) ν(C=O) 1605 (s) (^{12}C material); Elemental Analysis for $C_{31}H_{71}GeN_3O_3P_2PtSi_4$ unobtainable, product rapidly loses CO_2.

$(Et_3P)_2PtN(Ph)C(O)N(Ph)OGe[N(SiMe_3)_2]_2$ (9a). **3a** (50 mg, 0.06 mmol) was dissolved in 0.25 mL of C_6H_6. PhNCO (5 µL, 0.06 mmol) was added to the unstirred solution. After 40 min crystals began to form. The crystals were collected by reduced pressure filtration under nitrogen to yield 33 mg of **9** (59% isolated yield). ^{1}H NMR (CDCl$_3$) δ 0.16 (br, 36H, Si(CH$_3$)$_3$), 0.98 (m, 9H, CH$_2$CH$_3$), 1.14 (m, 9H, CH$_2$CH$_3$), 1.48 (m, 3H, CH$_2$CH$_3$), 1.87 (m, 3H, CH$_2$CH$_3$), 2.05 (m, 3H, CH$_2$CH$_3$), 2.29 (m, 3H, CH$_2$CH$_3$), 6.60 (t, aromatic), 6.84 (t, 1H, aromatic), 6.97 (t, 1H aromatic), 7.13 (t, 2H, aromatic), 7.15 (d, 2H, aromatic), 7.38 (t, 2H, aromatic), 7.88 (t, 2H, aromatic); ^{13}C NMR (CDCl$_3$) δ 166.6 (d, $^3J_{P-C}$ = 2.4 Hz, C=O), 151.9 (s, quaternary aromatic), 145.4 (s, quaternary aromatic), 128.5 (s, aromatic), 127.5 (s, aromatic), 127.2 (s, aromatic), 123.4 (s, aromatic), 122.0 (s, aromatic), 119.0 (s, aromatic), 20.0 (m, CH$_2$CH$_3$), 16.1 (m, CH$_2$CH$_3$), 9.62 (m, CH$_2$CH$_3$), 8.24 (s, Si(CH$_3$)$_3$), 7.94 (s, Si(CH$_3$)$_3$), 7.59 (s, Si-(CH$_3$)$_3$), 7.34 (s, Si(CH$_3$)$_3$); ^{31}P{^{1}H} NMR (CDCl$_3$) δ 6.1 (d w/ ^{195}Pt satellites, $^1J_{Pt-P}$ = 3377 Hz, $^2J_{P-P}$ = 19.0 Hz), −14.2 (d w/^{195}Pt satellites, $^1J_{Pt-P}$ = 1851 Hz, $^2J_{P-P}$ 19.0 Hz); IR (KBr) 1616 (vs) cm^{-1}, ν(C=O); Elemental Analysis Calcd for $C_{37}H_{76}GeN_4O_2P_2PtSi_4$: C, 42.28; H, 7.29; N, 5.33. Analysis C, 41.79; H, 6.79; N, 5.07.

X-ray Crystal Structure Determinations. Crystals were mounted on a glass fiber with paratone N hydrocarbon oil. X-ray data for **6a**, **7a**, and **9a** were collected on a Siemens SMART diffractometer with a CCD area detector equipped with a normal focus Mo-target X-ray tube (λ = 0.71073 A) operated at 2000 W power (50 kV, 40 mA). A total of 2132 frames were collected with a scan width of 0.3° in ω and an exposure time of 30 s/frame. The frames were integrated with Siemens' SAINT software package with a narrow frame algorithm. The structures were solved and refined with the Siemens SHELXTL (version 5.03) software package. The data were corrected for absorption using an empirical method (SADABS). X-ray data for **3a** was collected on a Siemens R3/v automated diffractometer with graphite monochromatized Mo Kα radiation (λ = 0.71073 Å) and solved by using direct methods with the program SHELXTL PLUS. All non-hydrogen atoms were allowed to refine anisotropically, with hydrogen atoms placed in idealized positions. Table 1 provides a general summary of crystallographic parameters. Specific data for each structure follows.

$C_{30}H_{71}GeN_3OP_2PtSi_4$ (3a). An orange crystalline plate of dimensions 0.18 × 0.22 × 0.44 mm was mounted and placed in a cold stream of nitrogen at 178(2) K. Additional details: Scan method ω, scan rate variable 2−5°/min, background-to-scan ratio 0.5, ω scan range 5−52° (h: −52/47; k: 0/14; l: 0/23), 10 081 measured, merged to 8354 unique reflections, R_{int} = 0.0607 empirical absorption correction.

$C_{33}H_{70}GeN_3O_3P_2PtSSi_4$ (6a·3C$_6$H$_6$). A small, colorless rectangular crystal (dimensions = 0.12 × 0.19 × 0.42 mm) was mounted and placed in a cold nitrogen stream at 158(2) K; the detector was placed at a distance of 4.577 cm from the crystal. The integration of the data using a primitive orthorhombic unit cell yielded a total of 174 787 reflections to a maximum of 2θ value of 58.64° of which 46 937 were independent and 36 887 were greater than $2\sigma(I)$. The final cell constants were based on the xyz centroids of 8192 reflection above $10\sigma(I)$. Analysis of the data showed negligible decay during data collection. Transmission coefficients ranged from 0.597 to 0.831. The structure was solved in the space group $Pna2_1$ with Z = 16 for the formula $C_{33}H_{70}GeN_3O_3P_2SSi_4Pt$. The final full matrix refinement based on F^2 converged at R1 = 0.0934 and wR2 = 0.1250 (based on all data); the largest peak in the final difference map was 2.254 Å and was associated with the Pt.

$C_{34}H_{76}GeN_3O_2P_2PtSi_4$ (7a·C$_6$H$_6$). A colorless rectangular block having dimensions 0.14 × 0.24 × 0.30 mm was mounted and placed in a cold nitrogen stream at 158(2) K; the detector was placed at a distance of 5.057 cm from the crystal. The integration of the data using a triclinic cell yielded a total of 90 474 reflections to a maximum 2θ value of 59.8° of which 44 710 were independent and 13 435 were greater than $2\sigma(I)$. The final cell constants were based on the xyz centroids of 7856 reflection above $10\sigma(I)$. Analysis of the data showed negligible decay during data collection. Transmission coefficients ranged from 0.417 to 0.831. The structure was solved in the space group $P\bar{1}$ with Z = 4 for the formula $C_{34}H_{76}GeN_3O_2P_2PtSi_4$. The final full matrix refinement based on F^2 converged with R1 = 0.0729 and wR2 = 0.1627 (based on observed data); R1 = 0.1102 and wR2 = 0.1737 (based on all data); the largest peak in the final difference map was 5.9 Å and was associated with Pt.

$C_{46}H_{85}GeN_4O_2P_2PtSi_4$ (9a·1.5C$_6$H$_6$). A small, colorless rectangular blocklike crystal (dimensions = 0.34 × 0.20 × 0.20) was mounted and placed in a cold stream of nitrogen on the diffractometer at 153(2)

K; the detector was placed at a distance of 4.577 cm from the crystal. Integration of the data using a primitive monoclinic unit cell yielded a total of 48 663 reflections to a maximum of 2θ value of 64° of which 17 097 were independent and 12 687 were greater than $2\sigma(I)$. The final cell constants (Table 1, XYZ) were based on the xyz centroids of 8192 reflection above $10\sigma(I)$. Analysis of the data showed negligible decay during data collection. Transmission coefficients ranged from 0.629 to 0.928. The structure was solved in the space group $P2(1)/c$ with $Z = 4$ for the formula $C_{46}H_{85}N_4O_2P_2Si_4GePt$. The final full matrix refinement based on F2 converged at R1 = 0.0748 and wR2 = 0.1239 (based on all data); the largest peak in the final difference map was 2.97 Å and was associated with the Pt.

Variable Temperature (VT) NMR Spectra of 3b. VT-NMR spectra of **3b** were recorded in toluene-d_8 on a Varian AMX-400 spectrometer at 399.967 MHz. Temperatures were measured by means of a thermocouple mounted in the spectrometer probe and calibrated to accuracy within ±0.1 °C. At each temperature increment, the instrument was reshimmed after the sample had equilibrated for 10 min. Line shape analysis of the obtained data was determined by manual measurements of the fwhm with caliper calibrated to +0.001 mm. The obtained spectra and tabulated rate measurements are included in the Supporting Information.

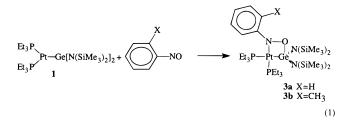**Attempted Reaction of 2,4,6-Tri-*tert*-butylnitrosobenzene with 1.** A flame sealed NMR tube was charged with 12 mg (0.015 mmol) of **1** co-mixed with 4 mg (0.015 mmol) of 2,4,6-tri-*tert*-butylnitrosobenzene dissolved in 0.25 mL of C_6D_6. No immediate reaction was observed. The sample was then heated in an oil bath to 80 °C for 2 h. Analysis of the tube by NMR spectroscopy showed no reaction as evidenced by the presence of only starting materials.

Attempted Reaction of *N*-Nitrosodimethylamine with 1. In the same manner as above, 35 mg (0.042 mmol) of **1** was allowed to react with 3 μL (0.041 mmol) of *N*-nitrosodimethylamine. At 20 °C, the NMR spectrum showed no reaction as evidence by presence of unreacted starting material. Heating the tube to 80 °C for 2 h also failed to induce reaction.

Attempted Reaction of Dimethylacetylenedicarboxylate (DMAD) with 3a. DMAD (1 equiv) was allowed to react with 50 mg (0.06 mmol) of **3a** dissolved in 0.25 mL of C_6D_6. The NMR tube was fitted with a rubber septum and protected from light with aluminum foil. No reaction was observed over a period of 72 h at 20 °C as evidenced by the presence of unreacted starting material in the ^1H NMR spectrum.

Results and Discussion

Reaction of Nitrosobenzene and 2-Nitrosotoluene with $(Et_3P)_2PtGe[N(SiMe_3)_2]_2$. Nitrosobenzene (1 equiv) underwent rapid reaction at −50 °C with a toluene solution of **1** causing a color change from golden yellow to deep orange. After removal of volatiles, recrystallization from hexane gave an orange powder, $(Et_3P)_2PtN(Ph)OGe[N(SiMe_3)_2]_2$ (**3a**). 2-Nitrosotoluene reacts under the same conditions to form the analogous orange product, $(Et_3P)_2PtN(o\text{-Tol})OGe[N(SiMe_3)_2]_2$ (**3b**). Characterization of **3a** by ^1H, ^{13}C, and ^{31}P NMR spectroscopy indicated the presence of two inequivalent triethylphosphine ligands, suggesting the adoption of a square-planar geometry about the platinum as well as a single phenyl group and equivalent trimethylsilyl groups. The ^1H NMR spectrum of **3b** gave an analogous set of spectral features, but the resonance for the trimethylsilyl groups was very broad at 20 °C, suggesting a dynamic process on the NMR time scale. IR spectra revealed the absence of a N=O stretching mode for both complexes. In analogy to previously observed results for the reaction of carbon dioxide with **1**,[3] we assigned the structure as a four-membered metallacycle with N bound to Pt and O bound to Ge as indicated in eq 1. The decision regarding the orientation of the nitrosobenzene binding was based primarily upon steric considerations, as the opposite orientation would place the phenyl group in conflict with the bulky bis(trimethylsilyl)amide groups.
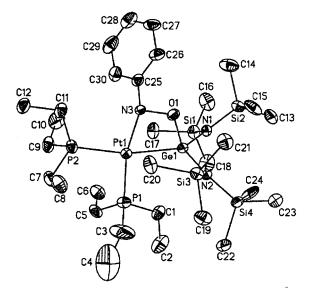

3a X=H
3b X=CH₃

(1)

Variable temperature NMR studies were used to explore the origin of the broad trimethylsilyl peak observed for **3b**.[10] Cooling a toluene-d_8 solution to −55 °C resulted in four sharp, distinct −SiMe₃ resonances. These peaks broadened as the solution was warmed, coalescing to a single, very broad feature at 25 °C. Upon heating the solution, two peaks began to grow out of the broad feature, resulting in two fairly sharp peaks at 60 °C. Continued heating to 105 °C resulted in a second coalesence to a single broad feature. Two separate dynamic events were determined to be present via line shape analysis of spectra collected between −55 and 105 °C. In the low-temperature region, the barrier was calculated to be 50 ± 2 kJ/mol. The barrier was observed to be associated with a conversion from two to four −SiMe₃ peaks and has been interpreted as the barrier to rotation of the Ge−N bond in this sterically hindered molecule. In the high-temperature region, the barrier was calculated to be 116 ± 1 kJ/mol and was assigned as the barrier to nitrogen inversion. The typical range of nitrogen inversion barriers previously observed is 175−313 kJ/mol,[11] considerably greater in energy than the barrier observed in this system. Although the role M−N bonding plays in the energy of nitrogen inversion is not well understood, the low barrier observed is consistent with the trend toward planar nitrogen typically observed for this class of complexes (*vida infra*). This assignment is further supported by the observation of both R and S isomeric products in the crystallographic analysis of **3a** (*vida infra*). Attempts to observe the nitrogen inversion barrier in **3a** by NMR spectroscopy were unsuccessful, although some broadening of the −SiMe₃ peak was observed upon cooling to −90 °C. The dramatic difference in dynamic behavior between **3a** and **3b** is most likely related to the position of the 2-methyl group in **3b** which places it in direct steric conflict with the −SiMe₃ groups.
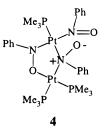
To assess the extent of activation of the nitroso group, and unambiguously assign the connectivity, single-crystal X-ray analysis of **3a** was obtained (Figure 1). As judged from the N−O bond distance of 1.498(6) Å, the nitrosobenzene is highly activated. This extremely long N−O bond is obtained in a system known to reversibly form metallacycles under very mild conditions.[3] It is interesting to note that this high degree of N−O activation, as judged by the N−O bond length, does not require highly oxophilic, irreversible reactions. The four-membered metallacycle displays noticeable distortion from planarity as evidenced by the 16° dihedral angle between the Pt−Ge and N−O bond vectors. Coordination about germanium resembles a distorted trigonal pyramid: the base formed by platinum and the nitrogen atoms bound to germanium and the cap formed by the oxygen of nitrosobenzene. Direct comparisons to a $(\mu\text{-}\eta^2\text{-nitrosobenzene-N})(\mu\text{-}\eta^1,\eta^1\text{-nitrosobenzene-N,O})$-$(\eta^1\text{-nitrosobenzene-}N)$tris(trimethylphosphine)diplatinum(II) (**4**)

(10) VT-NMR spectra are provided in the Supporting Information.

(11) For leading references into energetic issues in nitrogen inversion barriers, see: (a) Lehn, J. M. *Fortschr. Chem. Forsch.* **1970**, *15*, 311. (b) Nelsen, S. F.; Ippoliti, J. T.; Frigo, T. B.; Petillo, P. A. *J. Am. Chem. Soc.* **1989**, *111*, 1776. (c) Belostotskii, A. M.; Gottlieb, H. E.; Hassner, A. *J. Am. Chem. Soc.* **1996**, *118*, 7783.
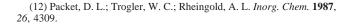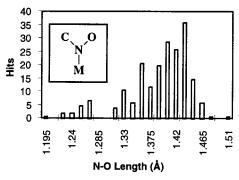
Figure 1. ORTEP of **3a** (50% probability). Bond lengths (Å) and angles (deg): Pt1−Ge1, 2.4214(7); Pt1−N3, 2.088(5); Pt1−P1, 2.249-(2); Pt1−P2, 2.356(2); N3−O1, 1.498(6); Ge1−O1, 1.820(4); Ge1−N2, 1.877(4); Ge1−N1, 1.884(4); C25−N3, 1.381(7); O1−Ge1−Pt1, 84.55(13); N3−Pt1−Ge1, 66.00(13); N3−Pt1−P2, 97.32(13); P1−Pt1−P2, 96.08(6); O1−N3−Pt1, 106.1(3); N3−O1−Ge1, 95.8(3); N1−Ge1−N2, 113.8(2) P1−Pt1−Ge1, 99.76(5); C25−N3−Pt1, 131.7(4); C25−N3−O1, 109.8(4); N1−Ge1−Pt1, 122.49(14); N2−Ge1−Pt1, 120.16(14); N1−Ge1−O1, 104.7(2); N2−Ge1−O1, 100.2(2).

4

Figure 2. Trogler et al. (μ-η^2-nitrosobenzene-*N*)(μ-η^1,η^1-nitrosobenzene-*N*,*O*)(η^1-nitrosobenzene-*N*)tris(trimethylphosphine)diplatinum-(II) (**5**).

complex synthesized by Trogler et al. containing three nitrosobenzene binding modes is instructive (Figure 2).[12] **4** contains one μ-η^2-nitrosobenzene with an N−O bond distance of 1.433(15) Å that bridges both Pt atoms in a binding mode similar to that observed for **3a**. The Pt−N interaction of 1.976-(11) Å is somewhat shorter than the 2.088(5) Å observed for **3a**. The Pt−O distance of 2.043(8) Å in **4** is somewhat larger than the 1.95 Å predicted by covalent radii; however, the Ge−O distance observed in **3a**, 1.820(4) Å, is slightly shorter than the 1.88 Å predicted by covalent radii. The weaker binding of the nitrosobenzene oxygen by Pt may be the key factor in the shorter N−O bond observed for the binding mode in **4**. Even the μ-η^1-nitrosobenzene of **4**, depicted as a formal zwitterion by Trogler et al., which has an N−O bond distance of 1.428(27) Å, is 0.070 Å shorter than **3a**. Prior to the synthesis of **3a**, **4** was noted to possess the longest N−O bond of any metal−nitroso complex.[12] Based on this comparison, one might have expected the charge distribution in **3a** to make the nitrogen atom quite electrophilic. However, the insertion chemistry we have observed is consistent with a nucleophilic character generally observed for metal-bound nitroso compounds. The N−O bond length in a more standard square-planar Pt nitroso complex such as $(Ph_3P)_2Pt(\eta^2\text{-ONPh})$

(12) Packet, D. L.; Trogler, W. C.; Rheingold, A. L. *Inorg. Chem.* **1987**, *26*, 4309.

Figure 3. Histogram of N−O bond lengths having the connectivity shown in inset.

(**5**) of 1.410(7) Å, is significantly shorter than found in **3a**. Figure 3 shows a histogram of N−O bond lengths compiled from a search of the Cambridge Structural Database (CSD) for N-bound metal complexes.[13] Examination of the resulting histogram reveals that most N−O bonds having this connectivity lie within 1.315 and 1.470 Å (91%). Only the N−O bond of **3a** exceeds 1.480 Å. The degree of pyramidalization observed for the nitrogen center is also quite rare. A search of the CSD for all M−N(R)O− derivatives finds that of the 89 complexes crystallographically characterized to date, the sum of the three nitrogen angles is generally between 352 and 364° (85 examples). Four complexes, all ArNO molecules side-bound to a metal center via the NO moiety so as to form a three-membered ring, have a three angle sum between 288 and 296°.[6a,14] For these molecules, the very acute M−N−O angle internal to the three-membered ring provides one angle between 60 and 70°. The other two angles are approximately 109°. The three angle sum for complex **3a** is 348°, making it one of only five such complexes characterized to data with a three angle sum less than 352°. **3a** can be described as a metallaoxaziridine, although all previous such complexes have contained ArNO side-bound to a single metal center. The pyramidizalization of the nitrogen atom in **3a** is probably related to the geometrical constraints imposed by the four-membered ring. Note that the similar μ-η^2-nitrosobenzene binding mode observed for **4**, forming a five-membered ring, gives an almost perfectly planar nitrogen atom with a three angle sum of 359.4°.[12]

Geoffroy et al. postulated that the reaction of $(CO)_5W{=}CR_2$ with PhNO forms a four-membered metallocycle intermediate on route to the observed ketone product and proposed metal−nitrene (Figure 4, pathway A).[15] Products were also observed supporting the presence of pathway B. To the best of our knowledge, **3a** represents the first isolated and characterized analogue of the proposed metallocycle intermediate. In contrast to the result for $(CO)_5W{=}CR_2$, **1** forms only one of the two possible metallacycles. The extremely long N−O bond suggests the metathesis observed for the carbene system may be poised to occur in the germylene system, and indeed, **3a** is both thermally and photochemically sensitive.[16] Unfortunately, efforts to trap potential metal nitrene and germanone species with dimethyl acetylenedicarboxylate, 2,3-dimethylbutadiene, and methyl-*tert*-butyl ketone were unsuccessful, and no products

(13) 3D search using the Cambridge Structural Database; Allen, F. H.; Kennard, O. *Chemical Design Automated News* **1993**, *8*, 31.

(14) (a) Liebeskind, L. S.; Sharpless, K. B.; Wilson, R. D.; Ibers, J. A. *J. Am. Chem. Soc.* **1978**, *100*, 7061. (b) Brouwer, E. B.; Legzdins, P.; Rettig, S. J.; Ross, K. J. *Organometallics* **1994**, *13*, 2088. (c) Ridouane, F.; Sanchez, J.; Arzoumanian, H.; Pierrot, M. *Acta Crystallogr. C* **1990**, *46*, 1407.

(15) Pilato, R. S.; Williams, G. D.; Geoffroy, G. L.; Rheingold, A. L. *Inorg. Chem.* **1988**, *27*, 3665−3668.

(16) The more sterically crowded **3b** has considerably more thermal stability. It does not begin to decompose until ~105 °C.

Arylnitroso Substrates on a Platinum−Germylene Complex

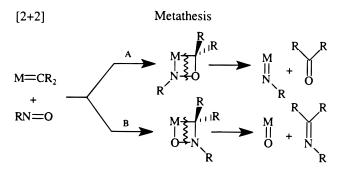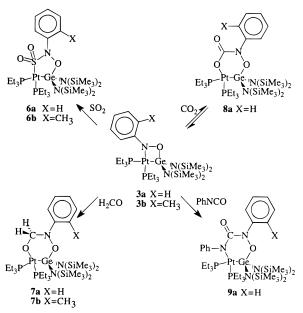*J. Am. Chem. Soc., Vol. 120, No. 30, 1998* 7489

[2+2]   Metathesis

Figure 4. Proposed metathesis mechanism for the reaction of arylnitrosocomplexes with metal carbenes.

could be isolated or identified. Related attempts to isolate the nickel analogues of **3a** and **3b** using $(Ph_3P)_2NiGe[N(SiMe_3)_2]_2$ (**2**) were unsuccessful, resulting in complex mixtures found to contain ∼4% of bis(triethylphosphine)azobenzene nickel (II), by comparison of NMR shifts to a known standard.[17] This product may result from a metathesis reaction similar to that proposed by Geoffroy but could also result from known oxygen atom transfer reactions that occur in Ni(0)/nitrosobenzene mixtures.[18] Attempts to synthesize other analogues of **3a** and **3b** were made. However, both 2,4,6-tri-*tert*-butylnitrosobenzene and *N*-nitrosodimethylamine failed to react with **1**, even when heated to 80 °C.

Insertion Reactions. A significant literature describing the coordination and reaction chemistry of C-nitroso-compounds exists.[19] An interesting and well studied class of reactions involves insertion into the Pt−N bond, primarily investigated for $(Ph_3P)_2Pt(\eta^2\text{-ONPh})$ **5**; where the behavior was attributed to nucleophilic attack by the nitroso-N.[6] Reagents observed to insert into **5** include PhNCO, CO_2, CS_2, benzylidenmalononitrile, tetracyanoethylene, benzaldehyde, and dimethylacetylene dicarboxylate. Since the binding modes of nitrosobenzene in **3a** and **5** were quite different, we pursued a series of insertion reactions to explore this class of reactivity in our system. Scheme 1 illustrates the chemical reactivity observed for **3a** with SO_2, H_2CO, PhNCO, and CO_2 and **3b** with SO_2 and H_2CO. Some general observations about each of the resulting heterocycles are informative. First, only dipolar substrates were observed to insert into the Pt−N bond to give ring expansion. As previously noted,[6] the most electropositive atom of the substrate's site of unsaturation undergoes nucleophilic attack by the nitroso nitrogen. Second, no evidence of attack at the Pt−Ge bond has been observed. Third, both five- and six-membered rings have been generated. The rings exhibit dynamic behavior at 20 °C in solution. The insertion reactions of SO_2 and H_2CO have not previously been observed for other M−nitroso complexes. In contrast to the behavior of the three-membered heterocycle **5**, no reaction was observed for **3a** or **3b** with dimethylacetylene dicarboxylate, acetaldehyde, or benzaldehyde.

Reaction of SO_2 with 3a and 3b. SO_2 (1 equiv) reacts readily with a stirred −78 °C toluene solution of **3a** resulting in an immediate color change from orange to light yellow. After removal of volatiles, the contents of the flask were extracted with a minimum of THF. Dropwise addition of an equal volume of Et_2O gave large colorless crystals over 24 h. The crystals displayed limited solubility in benzene and toluene yet were

Scheme 1. Insertion Reactions of **3a** and **3b** with SO_2, H_2CO, CO_2, and PhNCO

quite soluble in chloroform and THF. Characterization by ^1H, ^{13}C, and ^{31}P NMR spectroscopy indicated the presence of two inequivalent triethylphosphine ligands, suggesting the adoption of a square-planar geometry about the platinum as well as a single phenyl group. A broad single peak was observed for the −$SiMe_3$ groups, suggesting the presence of dynamic processes such as those discussed for **3b**. The IR spectrum revealed the presence of stretching modes attributable to an SO_2 functionality at 1384 and 1165 cm^{-1}. Elemental analysis confirmed the uptake of 1 equiv of SO_2. We originally believed that three structures for **6a** were possible: (1) SO_2 directly adding across the weakened N−O bond, (2) SO_2 directly adding across the Pt−Ge bond, or (3) SO_2 inserting into the Pt−N bond. The third structure was initially ruled out due to the lack of literature precedence for such reactions occurring with M−nitroso compounds. Results with CO_2 and other reagents gave us confidence that the Pt−Ge bond was not the site of insertion. Therefore we initially assigned the structure as SO_2 insertion across the weakened N−O bond in analogy to Cowie's proposal that SO_2 reacted with an elongated O−O bond in a four-membered metallacycle to generate a bridging sulfate complex.[20,21] Likewise, SO_2 was observed to reversibly insert into the N−N bond of $[Fe_2(CO)_6(\mu\text{-}N_2Ph_2)]$.[22]

To unambiguously determine the site and orientation of SO_2 incorporation, single-crystal X-ray analysis of **6a** was obtained (Figure 5). Surprisingly, SO_2 was found to insert into the Pt−N bond. The four independent molecules, possessing the connectivity portrayed in Scheme 1, were observed to have similar bond lengths, yet there existed two pairs of molecules varying significantly in terms of the N−O−Ge bond angle (101.4(5)° vs 108.1(5)°), inversion at nitrogen, and therefore ring confor-

(17) Ittel, S. D. *Inorg. Synth.* **1990**, 28, 98−104.

(18) (a) Otsuka, S.; Aotani, Y.; Tatsuno, Y.; Yoshida, T. *Inorg. Chem.* **1976**, 15, 656−660. (b) Berman, R. S.; Kochi, J. K. *Inorg. Chem.* **1980**, 19, 248−254.

(19) For a review, see: Cameron, M.; Gowenlock, B. G.; Vasapollo, G. *Chem. Soc. Rev.* **1990**, 19, 355−379.

(20) (a) Vaartstra, B. A.; Xiao, J.; Cowie, M. A. *J. Am. Chem. Soc.* **1990**, 112, 9425−9426. (b) Xiao, J.; Santarsiero, B. D.; Vaartstra, B. A.; Cowie, M. A. *J. Am. Chem. Soc.* **1993**, 115, 3212.

(21) Additional examples of SO_2 insertions into platinum-bound peroxides: (a) Horn, R. W.; Weissberger, E.; Collman, J. P. *Inorg. Chem.* **1970**, 9, 2367. (b) Valentine, J.; Valentine, D.; Collman, J. P. *Inorg. Chem.* **1971**, 10, 219. (c) Cook, C. D.; Jauhal, G. S. *J. Am. Chem. Soc.* **1967**, 89, 3066. (d) Farrar, D. H.; Gukathasan, R. R. *J. Chem. Soc., Dalton Trans.* **1989**, 557. (e) Bhaduri, S.; Johnson, B. F.; Khair, A.; Ghatak, I.; Mingos, D. M. P. *J. Chem. Soc., Dalton Trans.* **1980**, 1572.

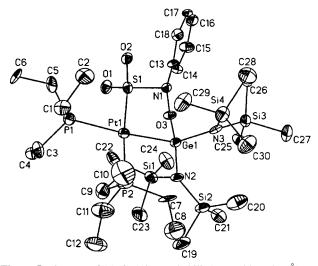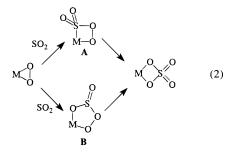(22) Kabir, S. E.; Ruf, M.; Vahrenkamp H. *J. Organomet. Chem.* **1996**, 512, 261−263.

Figure 5. ORTEP of (*S*)-**6a** (50% probability). Bond lengths (Å) and angles (deg): Pt1−Ge1, 2.4715(11); Pt1−P1, 2.373(3); Pt1−P2, 2.307-(3); Pt1−S1, 2.319(3); Ge1−N2, 1.889(8); O3−N1, 1.424(10); Ge1−O3, 1.861(7); Ge1−N3, 1.873(9); S1−O1, 1.478(8); S1−O2, 1.477(7); S1−N1, 1.778(8); N1−C13, 1.453(12); S1−Pt1−P1, 89.78(9); P2−Pt1−P1, 96.06(10); S1−Pt1−Ge1, 82.25(7); O1−S1−O2, 113.0(4); P1−Pt1−Ge1, 170.72(8); N1−S1−Pt1, 104.2(3); N3−Ge1−N2, 113.7-(4); N1−O3−Ge1, 101.4(5); O3−Ge1−Pt1, 98.2(2); O3−N1−S1, 106.6(5); O1−S1−Pt1, 114.0(3); O2−S1−Pt1, 114.5(3); O1−S1−N1, 107.8(4); O2−S1−N1, 102.0(4); S1−N1−C13, 115.1(6); O3−N1−C13, 110.3(7); N2−Ge1−O3, 99.0(3); N3−Ge1−O3, 99.7(3); N2−Ge1−Pt1, 116.1(3); N3−Ge1−Pt1, 123.0(3).

mation. The average N−O bond distance of 1.43 (1) Å is still quite long. The average N−S bond length of 1.78 (1) Å is longer than 98% of the previously characterized N−S bonds according to the Cambridge crystallographic database.[13] Platinum's coordination sphere resembles a distorted square plane comprised of cis-ligated triethylphosphines and a bidentate sulfoximido-germyl moiety.

The observation of SO_2 insertion into the Pt−N bond, as opposed to insertion into the N−O bond, provides the first isolated and characterized example of a metal-bound −S(O)₂N-(R)O− moiety, a species closely related to an elusive key intermediate proposed in the platinum-catalyzed Contact Process for the oxidation of SO_2 (eq 2).[7] Previous oxygen labeling experiments suggested that such insertion pathways should be considered because of the distribution of label in the final sulfate product. Collman et al. proposed intermediate species that did not contain a direct M−S bond such as B for the iridium complex used in their study, although species A could also account for the isotopic distribution observed.[21a,b]

(2)

To the best of our knowledge, no complexes have been isolated and structurally characterized to date containing the connectivity of elements outlined in intermediates A or B; however, **6a** is an isoelectronic analogue of intermediate A, albeit bridging over two metal centers. Given the apparent lack
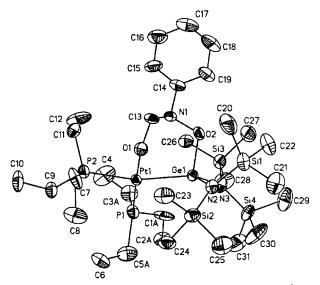

Figure 6. ORTEP of (*R*)-**7a** (50% probability). Bond lengths (Å) and angles (deg): Pt1−Ge1, 2.4874(9); Pt1−P1, 2.291(3); Ge1−O2, 1.909-(6); C13−N1, 1.500(12); Ge1−N2, 1.929(7); Pt1−O1, 2.106(7); Pt1−P2, 2.384(2); O2−N1, 1.476(9); O1−C13, 1.425(11); Ge1−N3, 1.952(8); N1−C14, 1.470(12); O1−Pt1−Ge1, 77.0(2); Pt1−O1−C13, 120.9(5); O1−C13−N1, 114.2(7); C13−N1−O2, 108.3(6); N1−O2−Ge1, 113.0(4); O2−Ge1−Pt1, 102.9(2); P1−Pt1−P2, 102.40(9); Ge1−Pt1−P1, 101.25(7); C14−N1−O2, 109.4(7); N2−Ge1−N3, 106.5(3); O1−Pt1−P2, 79.2(2); C14−N1−C13, 111.4(8); N2−Ge1−Pt1, 115.9-(2); N3−Ge1−Pt1, 127.6(2); N2−Ge1−O2, 98.9(3); N3−Ge1−O2, 99.4(3).

of any simple, homogeneous, structurally characterized analogues of the key Contact Process intermediates, the isolation of **6a** represents an interesting, although crude first model. The closest analogues previously structurally characterized were peroxodisulfate ions.[23] Unfortunately, we have been unable to observe interconversion of **6a** to an imido analogue of the metal−sulfate complex.

Reaction of H₂CO with 3a and 3b. Paraformaldehyde was allowed to react with a stirring benzene solution of **3a**. Reaction progress was monitored visually by disappearance of the initial orange color. The product was isolated by filtration from excess paraformaldehyde and was recrystallized from pentane as an off-white powdery solid. IR spectroscopy revealed the absence of a C=O stretch, and ¹H and ¹³C NMR data indicated that a single formaldehyde molecule had been complexed. Cis-inequivalent triethylphosphine ligands, a single phenyl ring, an upfield shifted methylene carbon, and no observable Pt−C coupling led us to assign the structure indicated in Scheme 1 for **7a**. Note that this is also consistent with the general observation that the nitroso-*N* acts as a nucleophile in the insertion reaction. Reaction of paraformaldehyde with **3b** gave the analogue **7b**.

X-ray crystallographic analysis of **7a** confirmed our structural assignment (Figure 6). Two independent molecules were observed in the crystal lattice. The dissymmetric isomers are nonsuperimposable mirror images differing by a ring flip with inversion at the ring nitrogen. The overall structure can best be described as a six-membered heterometallacycle possessing a cyclohexane-like boat conformation. The boat conformation avoids the 1,3-diaxial strain that would exist between the phenyl ring and the bulky −N(SiMe₃)₂ moiety of germanium in the chair conformation. **7a** is noteworthy as it is the first well characterized example of an aldehyde inserting into a metal-C-nitroso-compound leading to an O-bound hydroxamate-like moiety.

Reaction of CO_2 with 3a. A 10-fold excess of 10% $^{13}CO_2$/CO_2 was condensed into an NMR-tube containing a d_6-benzene solution of **3a**. The tube was flame sealed, and upon thawing rapid clarification of the initially orange solution was observed. ^1H, ^{13}C, and ^{31}P NMR spectroscopy indicated quantitative conversion to a new complex which possessed cis-inequivalent triethylphosphine ligands, a new set of phenyl resonances, and an upfield shifted trimethylsilyl singlet. The IR and ^{13}C NMR spectra revealed a carbamate-like C=O was present at 1605 cm^{-1} and 161.5 ppm, respectively. As in the cases of **7a** and **7b**, no ^{195}Pt satellites were observable, suggesting the absence of a direct Pt–C bond. To examine this phenomenon, we synthesized and structurally characterized a complex containing a bridging carbonate adduct which should possess a $^2J_{Pt-C}$, $(Et_3P)_2Pt(O^{13}C(O)O)Ge[N(SiMe_3)_2]_2$ (**10**), to serve as a model for $^2J_{Pt-C}$ constants in these systems.[24] The ^{13}C NMR spectrum of concentrated samples of **10** were unable to detect the presence of two-bond ^{195}Pt satellites. Given this close comparison, the absence of ^{195}Pt satellites in **8a** is not surprising. Attempts to isolate and structurally characterize **8a** were thwarted due to the rapid loss of CO_2 during workup, indicating reversible complexation. Based upon the spectroscopic evidence, and the chemical analogies presented in this paper, we assign the product of this reaction as shown in Scheme 1 for **8a**.

Reaction of PhNCO with 3a. To an unstirred benzene solution of **3a**, 1 equiv of PhNCO was added by syringe. After 40 min, the clarified solution began to form colorless crystals. The long, thin hexagonal plates were collected by filtration, washed with benzene, and dried in vacuo. Characterization by IR spectroscopy revealed urea-like C=O stretching frequencies at 1616 and 1588 cm^{-1}. ^1H, ^{13}C, and ^{31}P NMR spectroscopy gave evidence of cis-inequivalent triethylphosphines ligated to platinum, two inequivalent phenyl rings, and an intact germylene moiety. Given the presence of the intact C=O, we assigned the structure as shown in Scheme 1 for **9a** which resembles an N-bound urea fragment spanning the Pt–Ge–O fragment. To unambiguously assign the connectivity as well as to confirm the presence an intact Pt–Ge bond, analysis by single-crystal X-ray diffraction was obtained. An ORTEP diagram of **9a** is shown in Figure 7 with key bond lengths and angles. The six-membered heterometallacycle displays considerable distortion from planarity analogous to the boat conformer of cyclohexane rings. This conformation allows the phenyl rings to occupy a trans-configuration with respect to the Pt–Ge vector and minimizes 1,3 diaxial steric interaction with neighboring $N(SiMe_3)_2$ groups. Ligand coordination about platinum resembles a distorted square-planar environment. The Pt–N bond length of 2.112(3) Å is somewhat longer than the 2.088(5) Å observed for **3a**. Both N(1) and N(2) are planar as expected for nitrogen atoms bound to a carbonyl moiety.

The variation of the N–Ge–N bond angle in all of these structures is curious. In general, germylenes have Q–Ge–Q bond angles substantially less than the nominal 120° because of the large amount of s-character in the lone-pair and large amount of p-character in the ligand bonds.[25] Consistent with maintaining a germylene character, the N–Ge–N bond angle of **1** is 106.3(3)°.[3] Upon complexation of the nitrosobenzene to form **3a**, this angle opens up to 113.8(2)°. The four-
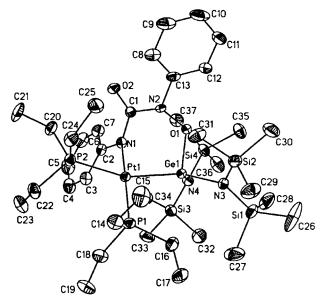

Figure 7. ORTEP of **9a** (50% probability). Bond lengths (Å) and angles (deg): Pt1–Ge1, 2.4562(5); Ge1–O1, 1.867(3); Ge1–N4, 1.883(3); Ge1–N3, 1.904(4); Pt1–N1, 2.112(3); Pt1–P1, 2.2692(11); Pt1–P2, 2.3776(12); N1–C1, 1.368(5); N1–C2, 1.411(5); N2–C1, 1.394(5); N2–O1, 1.405(4); N2–C13, 1.433(5); C1–O2, 1.237(5); N4–Ge1–N3, 105.6(2); O1–Ge1–Pt1, 99.44(9); P1–Pt1–P2, 94.48-(4); N1–Pt1–Ge1, 76.47(10); C1–N2–O1, 119.2(3); N2–O1–Ge1, 120.5(2); N1–Pt1–P2, 89.42(10); P1–Pt1–Ge1, 101.57(3); C1–N1–Pt1, 117.9(3); N1–C1–N2, 113.9(4); N4–Ge1–Pt1, 121.99(11); N3–Ge1–Pt1, 126.78(11); N3–Ge1–O1, 97.69(14); N4–Ge1–O1, 96.00-(14); Pt1–N1–C2, 119.1(3); C2–N1–C1, 119.7(3); N1–C1–O2, 126.0(4); O2–C1–N2, 120.0(4); C1–N2–C13, 122.2(3); C13–N2–O1, 111.1(3).

membered ring of **3a** contains a Pt–Ge–O angle of 84.55(13)°, thus considerable p-character is likely involved in ring-bonding, increasing the s-character in the Ge–N bonds. Insertion of SO_2 into **3a**, gives a five-membered ring complex **6a** in which this angle remains the same at 113.7(4)°. However, insertion of $H_2C=O$ or PhNCO to form six-membered rings **7a** and **9a** gives bond angles of 106.5(3)° and 105.6(2)°, respectively. This observation is consistent with an increase in the Pt–Ge–O bond angle to 102.9(2)° for **7a** and 99.44(9)° for **9a**. Other related structures published to date include a complex with no constraining ring, $(Et_3P)_2Pt(H)GeH[N(SiMe_3)_2]_2$. In this instance a N–Ge–N angle of 106.9(4)° is observed.[3] Another species that contains a four-membered ring, $(Et_3P)_2PtC(O)OGe-[N(SiMe_3)_2]_2$, exhibits a N–Ge–N bond angle of 110.0(3)°. Based on the trends discussed, the Pt–Ge–O angle for this complex would be expected to be between 85 and 105°. However, the experimentally determined value is 81.7(2)°,[3] even more acute than that observed for **3a**. Thus, although the bond angles can be rationalized for many of the structures as changes in the amount of p-character at Ge, this simple explanation does not suffice for all cases characterized to date. None of the other metrical parameters such as Pt–Ge or Ge–O bond distance correlate with the variation in N–Ge–N angle. The four-coordinate germyls present in all of these complexes adopt a roughly trigonal pyramidal geometry.

Conclusions

Arylnitroso compounds bind to group-10 metal–germylene complexes accompanied by an extremely lengthened N–O bond

(23) a) Harrison, W. D.; Hathaway, B. J. *Acta Crystallogr. B* **1980**, *36*, 1069. (b) Blackman, A. G.; Huffman, J. C.; Lobkovsky, E. B.; Christou, G. *J. Chem. Soc. Chem. Commun.* **1991**, 989.

(24) Litz, K. E.; Banaszak Holl, M. M. Unpublished results.

(25) (a) Fjeldberg, T.; Haaland, A.; Schilling, B. E. R.; Lappert, M. F.; Thorne, A. J. *J. Chem. Soc., Dalton Trans.* **1986**, 1551. (b) Grev, R. S.; Schaefer, H. F. *Organometallics* **1992**, *11*, 3489.

of 1.498(6) Å; currently the longest N−O bond of any M−nitroso complex. Chemical implications of the binding were explored using a series of Pt−N insertion reactions with SO_2, CO_2, H_2CO, and PhNCO which formed new S−N or C−N bonds. Despite the extremely lengthened N−O bond, the activations of dipolar substrates occurred only at the Pt−N bond and avoided cleavage of the N−O and Pt−Ge bonds. Thermal and photochemical reactions appearing to cleave the N−O bond resulted in a myriad of products. Insertion of SO_2 into the Pt−N bond of **3a** was particularly interesting because the platinum germylene provided the stabilization necessary to allow isolation and structural characterization of a model for a key step in SO_2 oxidation. Overall, these reactions highlight the ability of the Pt−Ge nexus to activate organic substrates to further modification. Contrary to the common situation observed for small molecule activations occurring at metal−metal bonds, the Pt−Ge interaction is robust and remains intact. Sufficient electrons are present in the Ge(II) ligand to promote continued ligation

to the platinum as a germyl fragment. We are pursuing chemistry designed to eliminate the nascent, novel heterocycles and regenerate $(Et_3P)_2PtGe[N(SiMe_3)_2]_2$ (**1**).

Supporting Information Available: Tables of crystal data, atomic coordinates, bond lengths and angles, anisotropic displacement parameters, and hydrogen coordinates and isotropic displacement parameters, VT-NMR spectrum, and N-inversion rates and rate of Ge−N rotation for **3b** (54 pages, print/PDF). See any current masthead page for ordering and Web access instructions.

JA980888F